Polymer Testing 134 (2024) 108440

Contents lists available at ScienceDirect

Polymer Testing

journal homepage: www.elsevier.com/locate/polytest

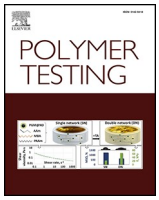

Feasibility assessment of polyvinyl alcohol-based bioresorbable cardiovascular stents manufactured via solvent-cast direct writing extrusion

Enric Casanova-Batlle [a], Samuel Montero-Coedo [a], Aniol Bosch [b], Antonio J. Guerra [b], Joaquim Ciurana [a,*]

[a] Product, Process and Production Engineering Research Group (GREP), Department of Mechanical Engineering and Industrial Construction, University of Girona, 17003, Girona, Spain
[b] EURECAT, Centre Tecnològic de Catalunya, Plaça de La Ciència 2, 08243, Manresa, Spain

ARTICLE INFO

Keywords:
Cardiovascular stent
Solvent-cast direct writing
Polyvinyl alcohol

ABSTRACT

Background: Bioresorbable stents represent a promising approach in cardiovascular interventions compared to drug-eluting stents. Additive manufacturing, particularly ink deposition, offers customization and versatility. This study delves into the potential of solvent cast direct-write 3D printing to fabricate cardiovascular stents using environmentally friendly solvents.

Methodology: Polyvinyl alcohol, a biocompatible synthetic polymer that dissolves in water, was investigated as a suitable material for stent fabrication. The polymer was deposited on a rotating mandrel and subsequently crosslinked to establish a pseudostable state. Test specimens and stents were fabricated for characterization of both the material and stent dynamics.

Results: This outcome is potentially suitable for deployment in the human body environment and adaptable to various biomedical applications, such as drug delivery patches or implants. The research optimized the fabrication of various stent geometries using polyvinyl alcohol and evaluated the kinetics of the working environment of these stents. Specifically, the 8-cell diamond stent showed remarkable characteristics, such as a high over-expansion of more than 0.5 mm, a compression force of 0.02 N and an elastic recovery of 88.85 %, with a strut thickness of 50.25 μm. Additionally, the study discusses the possibility of sterilizing polyvinyl alcohol with different methods, ethanol and autoclave were selected.

Conclusions: The results indicate that autoclaving leads to an increase in crystallinity. This yields a decrease in water absorption and an increase in mechanical properties. These results suggest that polyvinyl alcohol-based stents fabricated by solvent-cast direct writing are potential candidates for bioresorbable stent design.

1. Introduction

Cardiovascular stents are often implanted during percutaneous coronary interventions, standard procedure for the treatment of cardiac pathologies [1]. The purpose of cardiovascular stents is to open and widen clogged arteries. Currently, the gold standard is the drug eluting stents (DES) [2]. These stents are metallic coated with drug-eluting polymers. However, a new trend is emerging that seeks the dissolution of the coronary stent after the artery is healed. These stents are called bioresorbable stents (BRS) [3]. Typically to date, stent fabrication has been performed by laser cutting [4]. However, the emergence of additive manufacturing and the transition to BRS can result in the future of stents being disrupted by 3D printing. Additive manufacturing technologies offer a simple manufacturing technology, with no additional post-processing, with high efficiency to adapt to complex geometries [5]. Furthermore, as personalized medicine is expected to become more prevalent in the near future, 3D printing could play a crucial role in the pharmaceutical industry.

Guerra et al. pioneered tubular stent 3D printing using fused deposition modelling (FDM) technology [6]. From here, 3D stent printing has diversified from stereolithography (SLA), selective laser melting (SLM), ink deposition, etc [7–9]. FDM has emerged as a reliable and simple method for fabricating customized BRS stents. However, this technique depends on the availability of suitable filament materials. Besides, the current limitation of FDM remains in its resolution capability, as the thickness required for BRS often exceeds the capacity of the technology.

* Corresponding author.
E-mail address: quim.ciurana@udg.edu (J. Ciurana).

https://doi.org/10.1016/j.polymertesting.2024.108440
Received 13 March 2024; Received in revised form 17 April 2024; Accepted 25 April 2024
Available online 27 April 2024

This limitation can be mitigated using SLA and SLM additive manufacturing techniques, which offer resolutions down to 70 μm [10].

Although SLA presents a promising solution, uncertainty remains regarding whether photosensitive polymers will be approved for cardiovascular implants due to their questionable biocompatibility. On the other hand, although SLM offers adequate resolution and desirable mechanical properties, the selection of suitable materials for biodegradable options are limited. Among these technologies, solvent cast direct writing (SC-DW) ink deposition emerges as a compelling solution, mainly due to its inherent flexibility in ink customization. The main requirement is to find a suitable solvent for the polymers to be used. Therefore, creating a multi-material ink is a simple process if different materials are miscible in the same solvent. Then, once dissolved in the ink, it is possible to incorporate radiopaque agents or drugs. This capability not only serves the controlled release of drugs, but also increases the overall value of the stent [8]. Currently, stents manufactured by the solvent-cast-direct-writing technique use a copolymer combining PLLA and PCL. However, in this study the solvent used for polymer dissolution is chloroform. Despite its elimination by heat treatment, the search for more biocompatible alternatives is crucial. The use of chloroform-free solvents not only improves overall biocompatibility, but also makes the process safer for the operator in charge of stent fabrication. It also reduces the need for additional equipment, as the noxious gases associated with chloroform are eliminated.

Poly(vinyl alcohol) (PVA) is a water-soluble biomaterial whose solubility has been studied by different authors. Typically, its solubility depends on the molecular weight and degree of hydrolysis [11]. However, long term stability structures can be achieved by increasing the degree of crystallinity [12]. These crosslinking methods can be carried out by chemical methods, commonly crosslinked with formaldehyde or glutaraldehyde [13]. Further, physical methods such as the freeze-thaw or annealing approach can also be performed [14]. These methods yield to temporary water-insoluble structures that have been previously studied for biomedical applications [15]. While polymers such as PLA which gradually degrade and are absorbed into the body through the natural pathways, PVA requires chemical modification for use in the field of biodegradable medical devices. Consequently, researchers have explored the utilization of chemically modified PVA for fabricating biodegradable cardiovascular stents [16].

Furthermore, as PVA offers a nonlinear stress-strain profile remarkably similar to that of porcine arteries it has been widely used in the cardiovascular field [17]. On the premise of this property, other research groups attempted to fabricate cardiovascular stents by braiding PVA yarns. They concluded positive fibroblast proliferation at 72h [18]. Further studies were conducted using the PVA stents embedded subcutaneously within *in vivo* trials. The study suggested that PVA stents were non-toxic and biocompatible since after 28 days, the shape was maintained, indicating a good biological response [16].

In this regard PVA could be a promising candidate for stent manufacturing, since if a high level of crystallinity is achieved, it offers an ultimate tensile stress twice as high as compared to PLA [19]. This factor could be crucial because a key drawback of BRS is the low mechanical properties of the polymers used. This means that it can sustain a stress twice as high as the most used polymer for the manufacture of commercial BRS. In addition, the Young's modulus (E) can be increased by repeated temperature cycling. For example, freezing at −20 °C followed by thawing at 23 °C [17]. Moreover, as PVA is a polymer which is subject to hydrolysis within the body, thus it could be used for drug delivery purposes. Drug release assays with PVA films have been performed and it has been found that drug release can be controlled through the degree of crosslinking of the polymer [20].

This study represents a significant advance in the field by introducing a novel approach to address the challenges associated with stent fabrication using the SC-DW technique with an aqueous PVA solution printed on a tubular surface. Therefore, deionized water was used as an alternative to harmful solvents. The main objective was to provide a viable alternative to cytotoxic solvents, such as chloroform, in stent fabrication with this method. The research systematically tuned SC-DW technology to enable 3D printing of PVA, with potential implications for drug delivery and providing opacity in stent applications, without the use of toxic solvents. In addition, this study evaluated the mechanical and degradation properties of PVA fabricated using the proposed method. The investigation included an optimization of the printing parameters which was used to print various stent geometries. Subsequently, an analysis of the expansion and compressive strength of the printed stents was conducted. Finally, to ensure practical applicability, various sterilization methods were employed. Then, to determine the characteristics of the different sterilization methods, the material was tested by dynamic mechanical analysis (DMA), its crystallinity was evaluated by differential scanning calorimetry (DSC) and a degradation test was performed.

2. Materials and methods

2.1. 3D printing system

The printing system used was based on the 3D axis printing technology with a rotating mandrel presented in previous studies [6]. Specifically, in this study the printing head was replaced by a 1 mL Luer-Lok Tip syringe (BD, USA). The ink was ejected from the syringe through a mechanical piston that controlled the volume inside the reservoir, Fig. 1. The ink was extruded through a precision G21 gauge needle (Nordson EFF, USA) which had an inner diameter of 0.51 mm. The fabrication of the stents was conducted at 25 °C during the whole process.

2.2. Preparation of the ink

PVA powder (Sigma Aldrich, USA) was mixed with miliQ water at a ratio of 28 % (w/v). It was left at 135 °C overnight under stirring. It was stored at room temperature and preheated to 50 °C thus facilitating its introduction into the printing syringe. Further details of the PVA employed can be found in Table 1.

2.3. Parameterization of the parameters with dimensional features

A two-parameter factorial design of experiments with 4 levels was used to parameterize the printing parameters with the dimension of the printed lines (N = 3). The selected manufacturing parameters were the printing speed d (PS: 100–400 mm/min) and the flow rate at which the material is extruded (FR: 100–200 %). The analyzed parameters were detailed in Table 2.

A 40-mm line of the parameter combinations indicated in Table 2 were printed. The width of the lines was calculated with a Micromar 40EWV micrometer (Mahr, Germany) at 3 points (distal, proximal and middle). The mean of these data was declared as the line width score. Then, the mean values were used to create a regression model (Matlab, USA).

2.4. Stent geometry

The stent model selected for the study was a diamond-shaped closed cell stent, Fig. 2-d. Three different stent designs were designed, maintaining the geometry while modifying the cell density, Fig. 2 a-c. Parameters to achieve a 0.51 mm strut width (S_W), corresponding to the inner diameter of the G21 tip, were calculated using the model obtained. The parameters of $P_S = 450$ mm/min and $F_R = 2$ μL/mm were selected. Additionally, Table 3 shows the detailed parameters of inner diameter ($I_\varnothing$), number of cells (N_C), S_W, hinge width (H_W), cell width (C_W), cell length (C_L) and the cell area (C_A).

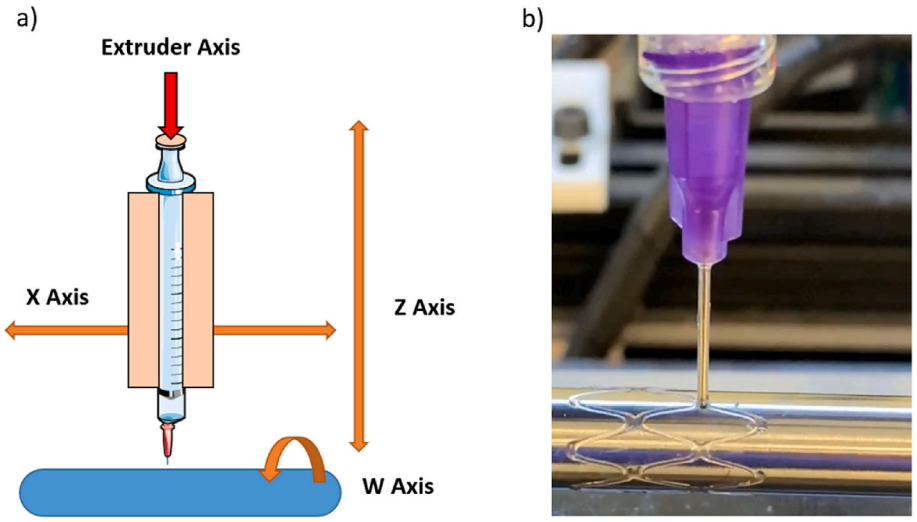

Fig. 1. a) Conceptual machine configuration. b) PVA stent printed with a G21 tip.

Table 1
Material properties.

Material density	Melting temperature	Molecular weight (M_W)	Young Modulus (E)
1,19 g/cm^3	200 °C	89000–98000 Da	707.9 MPa

Table 2
Two-parameter factorial design levels.

Levels	1	2	3	4
P_S (mm/min)	100	200	300	400
F_R (μL/mm)	5	6	7	8

2.5. Characterization of the manufactured stents

The feasibility of the fabricated stents was evaluated both in terms of their dimensional properties and their expansion and compression dynamic behavior.

2.5.1. Dimensional features

The dimensional characteristics of the fabricated stents (S_W, H_W and

Table 3
Theoretical stent model parameters.

$I_\varnothing$	N_C	S_W	H_W	C_W	C_L	C_A
5 mm	17	0.51 mm	1.02 mm	9.60 mm	3 mm	15.85 mm^2
5 mm	38	0.51 mm	1.02 mm	7.00 mm	2.77 mm	11.22 mm^2
5 mm	48	0.51 mm	1.02 mm	6 mm	2.20 mm	8.14 mm^2

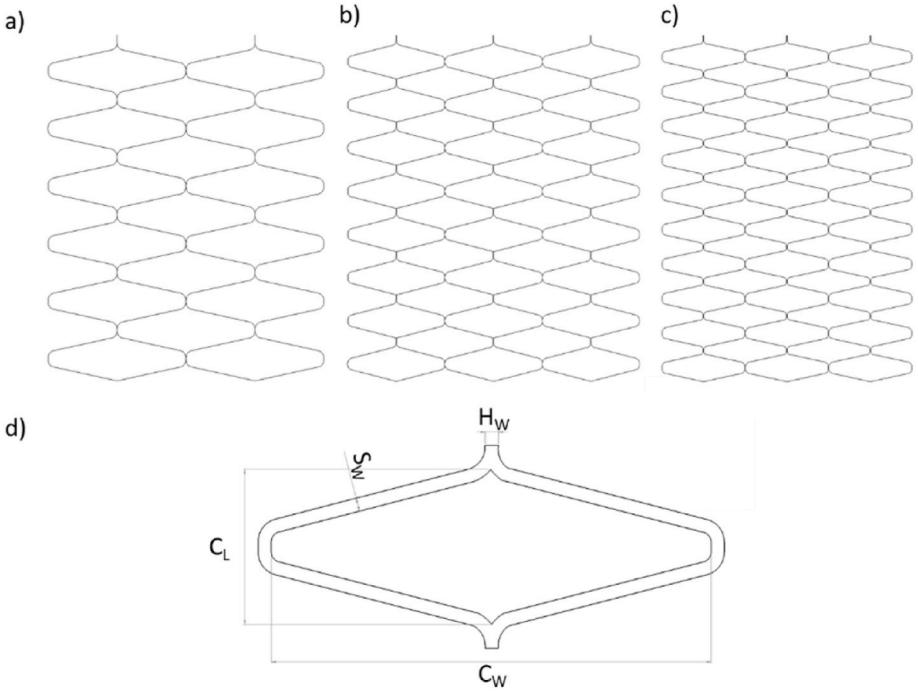

Fig. 2. a-c) Complete stent geometry shape design for the fabrication. d) Stent cell geometry.

C_A) were analyzed. A ZEISS discovery v12 stereo microscope coupled to the Invenio 20EIII microscope digital camera (5 megapixels) was used. Matlab was employed to process the images and collect the data. Two images were taken from the different replicates (N = 5).

2.5.2. Expansion test

A tool was designed that progressively increased the diameter of the stent to see the expansion capacity of the stents. The tool started at the stent manufacturing diameter (5 mm) and gradually increased, 0,5 mm for each step. All stents (N = 5) were inserted on the proximal side and by a rotary motion were moved to the upper diameters. These were expanded to the step prior to the rupture. The stent was then removed and after 300 s the recoil was measured at 30 and 300 s with a Micromar 40EWV micrometer (Mahr, Germany).

2.5.3. Compression test

A compression resistance parallel plate test was performed in order to measure stents' radial strength, following the methodology commonly employed by other research groups in the field (Fig. 3) [7,8,21]. Stents were compressed using a Discovery HR-2 rheometer equipped with a load cell of 50 N (TA instruments, USA) with the upper plate advancing towards the lower plate at 1 mm/min following ISO 25539-2 (N = 5) [22]. At 50 % reduction in diameter, radial force was noted and determined as the axial force.

2.6. Characterization of the material after sterilization

Test specimens were manufactured by extruding the material through the tip by the same procedure as during printing. The test specimens for the degradation tests consisted of circular samples of 10 mm diameter by 0,5 mm thickness. As for DMA test specimens, they were made rectangular (20 × 5 x 0,5 mm).

These samples were sterilized by different methods.

- Following the laboratory sterilization protocol previously reported in other studies, samples were subjected to overnight sterilization in ethanol, followed by an additional 30 min of ultraviolet exposure [23]. The test specimens were sterilized by immersing the material in absolute ethanol (Panreact, Spain) for 24h. Ethanol removal was performed through aspiration followed by two rinses with PBS (Gibco, USA).
- Standard autoclaving procedures were followed, autoclaving for 15 min at 121 °C in humidity 90 % and 30 min at dry temperature. The autoclaving method was evaluated by analyzing the effects of one and two autoclaving cycles.

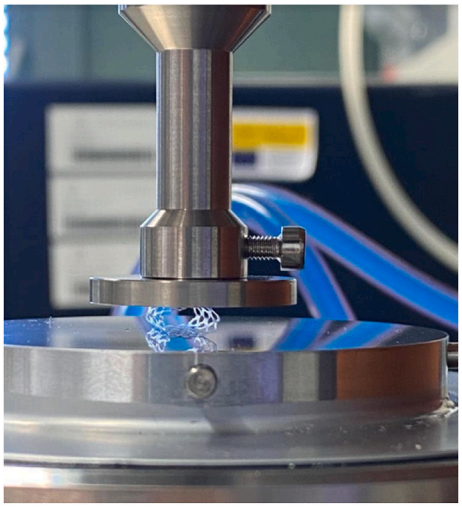

Fig. 3. Compression test assay for Stent evaluation.

2.6.1. DMA

A Mettler Toledo DMA/SDTA 861 equipped with dual cantilever tools was used to perform the DMA analysis. The test was run with a preload of 1 N and a frequency of 1 Hz. The samples were heated from 0 to 230 °C at 5 °C/min in an air atmosphere (N = 2).

The thermal properties of the obtained specimens were assessed by means of differential scanning calorimetry using a TA Instruments DSC Q2000 in order to evaluate the influence of the sterilization process on the crystallinity. Scans were run from 30 to 305 °C at a heating rate of 10 °C/min. The test was performed in an inert atmosphere with a nitrogen flow rate of 50 ml/min.

The degree of crystallinity (X_C) of PVA was calculated by the equation described by Hassan and Peppas, which is as follows [11]:

$$X_C = \left(\frac{\Delta H_m}{\Delta H_0}\right) x\ 100 \qquad \text{Eq. 1}$$

Where ΔH_m is the melting heat of the PVA sample and ΔH_0 is the melting heat of fully crystalline PVA. The heat, required for melting of fully crystalline PVA, is 138.60 J/g [24].

2.6.2. In vitro degradation test

To analyze the water absorption and short-term degradation of the manufactured stents, an *in vitro* assay in PBS was performed. The two different sterilization methods described above were used to evaluate the effect of the weight loss (W_L) and water absorption (W_A) on the sterilization of the material.

Circular test specimens of 10 mm of diameter and 0,5 mm of thickness were fabricated with 28 % (w/v) PVA solution by the solvent cast method. Evaporation of water was conducted at 37 °C for 24 h. Then, the test specimens were sterilized. Samples were weighed with a Sartorius ED224S analytical balance (Sartorius, Germany), and transferred to 24-well non-adherent cell culture plates (Sarstedt, Germany). 2 mL of PBS was added to each well and kept in incubator for 1 h, 4 h, 1 day, 4 days and 7 days.

The W_A rate was evaluated with equation (2):

$$W_A\% = \frac{W_w - W_d}{W_d} * 100 \qquad \text{Eq. 2}$$

The W_L percentage was estimated using equation (3):

$$W_L\% = 100 - \left(\frac{W_O - W_d}{W_O} * 100\right) \qquad \text{Eq. 3}$$

W_A and W_L were evaluated by weighing the samples on a weighting scale (Mettler Toledo Sartorius 2 MP Scale, USA), considering the sample's original weight after the sterilization process (W_0), weight of the wet sample (W_W), and residual weight after degradation once it had been completely dried (W_d) in an oven for 10 h at 75 °C.

3. Results

The PVA was optimized and successfully printed on a tubular printing surface using the SC-DW additive manufacturing approach. Then, based on the parameters found, the stents were effectively fabricated and subjected to several tests. Finally, the material was sterilized and evaluated for characterization of PVA inks printed at 28 % (w/v).

3.1. Optimization of the PVA printing ink for manufacturing

A linear regression model was calculated to fit the experimental data of the line width to the printing parameters with the function *fitlm* provided by Matlab. The t-statistic was calculated as the ratio of the coefficient estimate to its standard error. The p-value associated with each t-statistic evaluated the probability of observing a t-statistic as extreme as the one calculated, assuming the null hypothesis that the predictor had no effect. Parameters not influencing morphological

characteristics were removed from the model ($p < 0.05$). A linear model with interactions and quadratic coefficients was estimated. Each of the measured parameters (P_S and F_R) had a significant effect on the parameters analyzed, according to the following equations:

$$Line\ width\ (P_S, F_R) = 0.82 - 0.0009 * P_S + 0.05 * F_R \quad \text{Eq. 4}$$

Fig. 4 shows the experimental data listed in Table 2. Additionally, it depicts the interpolation of the model to obtain the parameters needed to achieve a line thickness consistent with the inner diameter of the tip used (0.51 mm). Thus, the parameters obtained from the model to satisfy the desired dimensions were 450 mm/min of P_S and 2 μL/mm in F_R. These parameters were selected for stent fabrication throughout this study.

3.2. Stent fabrication and dimensional assessment

Table 4 summarizes the morphological data of the fabricated stents obtained from the ZEISS discovery stereo microscope. The cardiovascular stents were grouped according to their N_C. The results were presented as mean values ± standard deviations. Cardiovascular stents with a N_C of 6 presented a mean S_W of 0,47 mm, very close to the modeled value (0.51 mm). However, the H_W of the stents was more than 3 times this value (1,67 mm). In addition, C_W and C_L values were 8,64 mm and 1,56 mm, respectively, being much lower than the expected theoretical target. By increasing the number of cells to 8, it was observed that S_W was 0,62 mm and H_W 2,68 mm, which represented a significant increase compared to N_C of 6. Consequently, C_W and C_L values decreased to 4,30 mm and 0,80 mm, respectively. Further increasing the cell size to 10 resulted in slightly higher S_W compared to the 8-cell N_C. S_W was measured at 0,64 mm, indicating a slight increase. H_W showed a similar trend. C_W and C_L values decreased to 3,13 mm and 0,75 mm, respectively.

Fig. 5 illustrates how the thickness expressed in the table can be reflected in the stent struts. It could be observed that in the straight trajectories the struts were thinner. However, in the curves they become thicker.

3.3. Stent dynamics - expansion and compression

The compression force values presented in Fig. 6 represent the amount of force applied to each group of PVA stents with different N_C during the compression test. The data show that the 6-cell stents

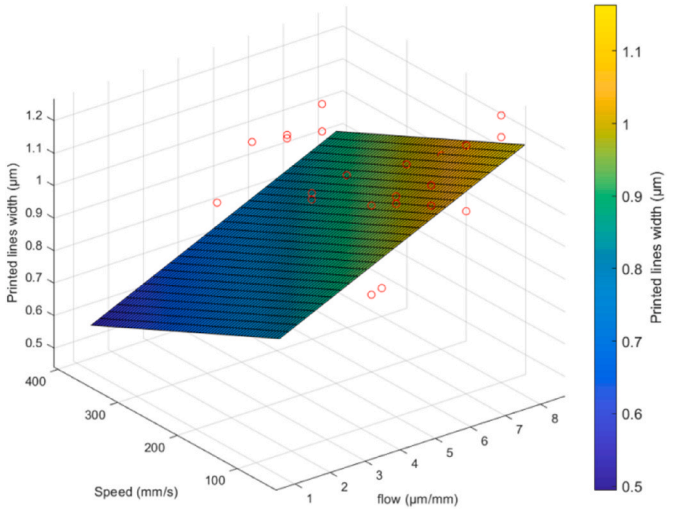

Fig. 4. Fitted Response Plot of the Regression Model. Red markers represent the experimental data, plotted according to the experimental model. (For interpretation of the references to colour in this figure legend, the reader is referred to the Web version of this article.)

Table 4
Stent dimensional parameters characterization with mean and standard deviation (N = 5).

$I_{Ø}$ (mm)	N_C	S_W (mm)	H_W (mm)	C_W (mm)	C_L (mm)	C_A (mm^2)
5	17	0,47 ± 0,09	1,67 ± 0,11	8,65 ± 0,18	1,57 ± 0,20	7,60 ± 0,50
5	38	0,62 ± 0,08	2,68 ± 0,32	4,30 ± 0,39	0,80 ± 0,13	4,63 ± 0,28
5	48	0,64 ± 0,07	3,26 ± 0,36	3,14 ± 0,31	0,75 ± 0,11	3,21 ± 0,26

experienced a lower compressive force of 0.0073 N, while the 6-cell dual-layer stent group and the 8-cell stent group both experienced a compressive force of almost 3 times higher, 0.019 and 0.02 N, respectively. The 10-cell stents experienced a slightly lower compressive force, 0.016 N.

The plastic strain values represented in Fig. 6 represent the amount of permanent deformation that occurred in each group of stents during the compression test, expressed as a percentage of the original dimensions. These values yield insights into the relative plasticity, or the ability of the stents in each group to undergo permanent deformation when they were subjected to compressive forces. The group of 6-cell stents with two layers was the one that exhibited the best results, presenting a recovery of 88.85 % of its original diameter. On the other hand, the values were lower although similar for the 8- and 10-cell stents where the stent recovered only 78.8 % and 79.1 % of its original diameter, respectively. Finally, the 6-cell stents presented a recovery of the original diameter of only 65.8 %.

In terms of expandability, Fig. 7 presents the expansion results obtained for the different stent geometries at each time interval. The measurements were presented as mean values. It could be observed that stent expansion varies according to the geometry chosen for the fabrication of the stent. It could be observed that the maximum expansion was reached by the 6-cell stent with a maximum diameter of 11,5 mm, while the 8- and 10-cell stents reached maximum diameters of 5,87 mm and 5,51 mm, respectively. After 30 s, the 6-cell stent had a diameter of 10,15 mm, representing a decrease of 11,74 % of the maximum diameter. On the other hand, the 8-cell stent and the 10-cell stent, presented a lower recoil in percentage, being less than 2 % in both cases.

Five minutes after expansion, the 6-cell stent showed a diameter of 9,63 mm, thus lowering the maximum expanded diameter a reduction of 16,26 %. On the other hand, the diameter of the 8-cell stent stabilized with an average diameter of 5,8 mm and the 10-cell stent maintained a diameter of 5,26 mm.

3.4. Sterilization-induced crystallization

Samples were made from the 28 % (w/v) PVA solution for the DSC test. Dehydration of the samples in an oven at 37 °C formed the PVA hydrogels. These were sterilized with ethanol or 121 autoclave cycles (1–2) to assess the sterilization response. Once sterilized, their thermal behavior was evaluated with DSC, Fig. 8.

Fig. 8 depicts the heat flow over the temperature interval from 20 to 250 °C. Two main events were observed. From ~85 °C onwards a thermal effect associated with the evaporation of moisture and possible residual water that might have been retained in the sample. Then a pronounced endothermic process associated with the melting of the material. It was integrated with respect to time for the calculation of the enthalpy of the melting process. With this parameter, as indicated by Eq. (1), the crystallinity was calculated, Table 5. It was observed that the crystallinity of the samples increased with the autoclaving process, being the 2 autoclaving cycles the process with a higher crystallinity as a final result.

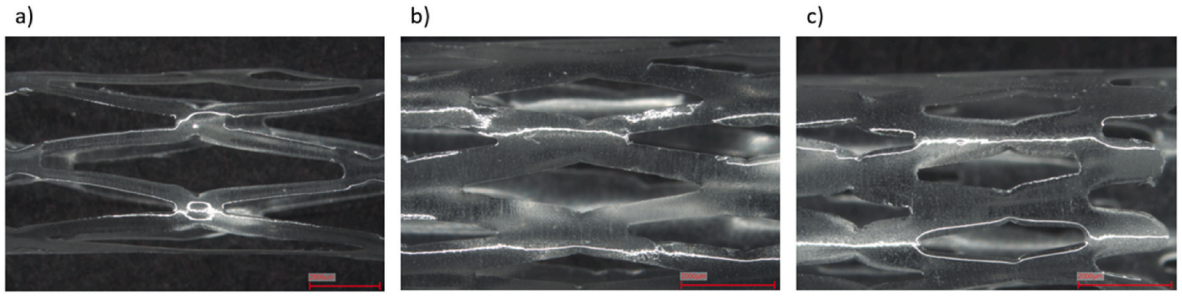

Fig. 5. Stent geometries. (a) Six-cell design, (b) Eight-cell design (c) Ten-cell design. These stents images were utilized to extract the data presented in Table 4, which characterizes their dimensional parameters.

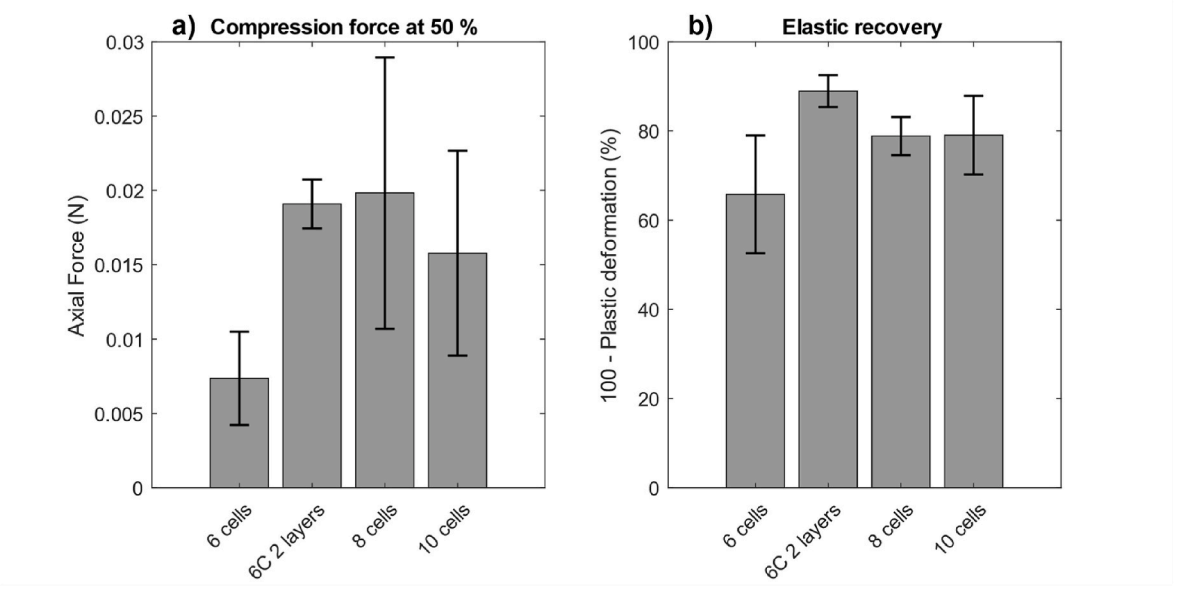

Fig. 6. Stents characterization at the compression test. a) Compression force at 50 % deformation for PVA stents with the different geometries and thickness. b) Elastic recovery shown by stents.

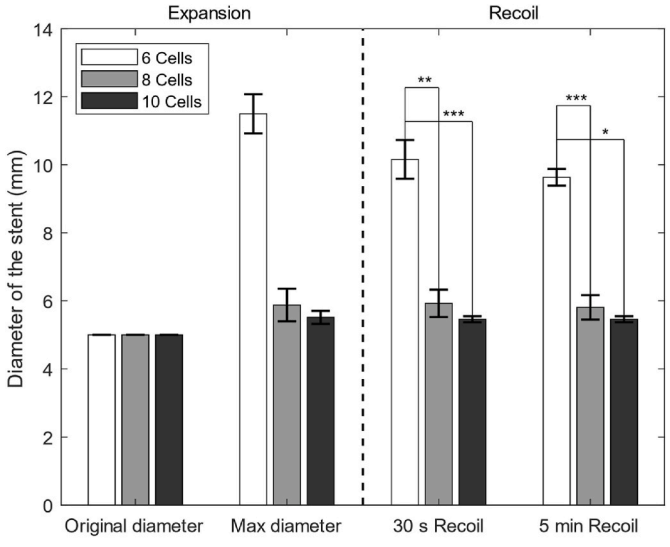

Fig. 7. Evolution of stent diameter during expansion test for different stent geometries.

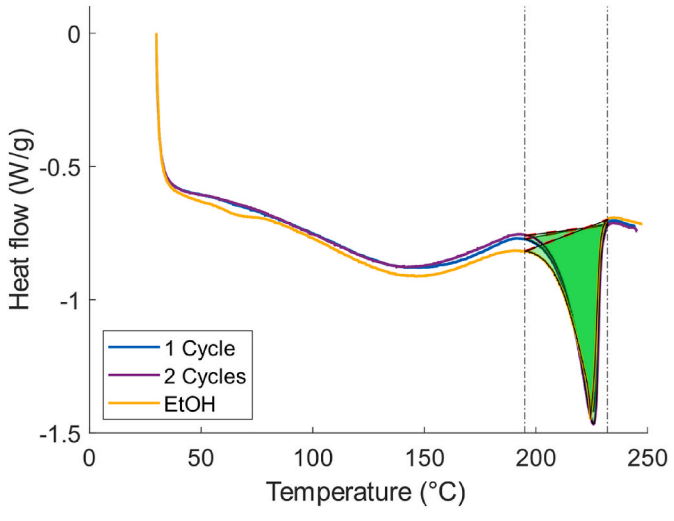

Fig. 8. DSC Analysis: Heat Flow on Temperature for Three Sterilization Methods. The heat flow was integrated over time during the melting event of PVA, in green. (For interpretation of the references to colour in this figure legend, the reader is referred to the Web version of this article.)

Table 5
Crystallization and glass transition temperature (T_g) calculations.

	Crystallization (%)	T_g (°C)
1 Cycle	40.27	52.35
2 Cycle	41.33	53.24
EtOH	38.67	52.22

3.5. DMA

Fig. 9 shows the results of the DMA test. It could be observed that the autoclave sterilization showed higher values of the storage modulus (E′) between 25 °C and 60 °C than those sterilized by the ethanol method. These values were 14.3 % higher when the samples were sterilized with 1 autoclave cycle. However, it could be observed that this value further increased when a second cycle was added to the PVA test specimens with an increase of 7.65 %. However, as the temperature increased, the values of E′ between the groups depicted similar behavior above 55 °C, tending to become lower as the temperature increased.

The values for the glass transition temperature (T_g) were calculated from the maximum peak of tan delta. It could be observed that the autoclaving cycles increased this value by 1.02 °C, compared to the 2 cycles autoclaving method and the ethanol-sterilized test specimens. In the case of 1 cycle of autoclave, T_g is found at a point between the two previous conditions.

3.6. PBS degradation and absorption kinetics

The circular solvent-cast PVA test specimens were immersed after their respective sterilization methods, ethanol immersion and autoclaving at 121 °C. Fig. 10-a shows that the PBS absorbance described the same profile for both conditions, a sharp PBS absorbance during the first hours. An abnormal peak was observed at 4 h for the EtOH sterilized conditions. This anomaly may be attributed to the method used, which encounters challenges in effectively removing surface water when weighing the wet sample. This was followed by saturation of the PBS absorbed at a value of 165,9 % and 64,5 % on average with ethanol and autoclaving respectively. Despite the similar behavior, it could be appreciated that the ethanol sterilized test specimens presented a higher PBS absorption, almost 3 times superior at 4 h from the beginning of the test and approximately twice as high during the saturation stage.

PVA has a partially crystalline and partially amorphous composition. The weight loss curve shows weight loss values reaching 11,1 % in the case of EtOH sterilization and 6,8 % in the case of autoclave sterilization

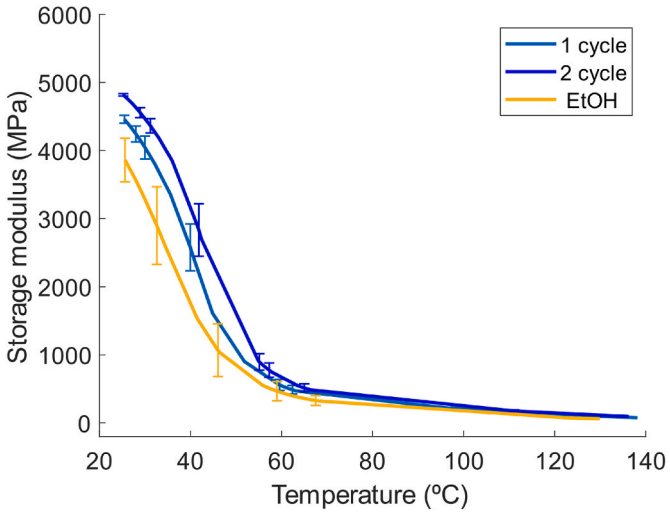

Fig. 9. DMA analysis, mean values and standard deviation of the storage modulus throughout the duration of the DMA test (N = 2).

at 4 days. Approximately half of the total weight lost was found in the first 4 h of the experiment. Then, both conditions had a tendency to reduce weight until the 4th day. At this time, a saturation of the degradation was observed, and it even seemed to increase, which was probably due to the variability between experiments.

4. Discussion

In this study, the fabrication of 28 % (w/v) PVA cardiovascular stents extruded by the SC-DW technique was evaluated, in terms of dimensional resolution, compression and expansion. In addition, the possibility of sterilizing the extruded PVA by various methods was evaluated in order to assess the effect on its mechanical properties, degradation kinetics and W_A, and lastly, on its crystallinity structure.

4.1. Stent properties and perspectives

Studies on PVA stents have investigated a spectrum of sizes, ranging from 3 mm to 18 mm [21,25]. However, cardiovascular stents typically range in diameter from 2.5 to 4 mm, while peripheral stents, designed for the treatment of cardiovascular disease, can reach up to 7 mm. To ensure versatility and scalability for cardiovascular and peripheral applications, stents with a diameter of 5 mm were manufactured in this study. The stents were printed with previously optimized parameters on a tubular surface with a single deposition layer to obtain a S_W of 0,51 mm. Remarkably, this parameter yielded accurate results for the 6-cell stents, S_W of 0,47 ± 0.09 mm. However, when analyzing the H_W results, it was observed that this value was higher than the predicted one. This deviation could be attributed to the extrusion of a viscous solution during the printing process on the curve trajectories. The material tends to fuse when the strut spacing is deposited too close, which is especially prevalent in the case of the hinges. Therefore, the initial optimization was performed for straight lines and resulted in several alterations when handling curved trajectories. This pattern was more evident in the case of stents manufactured with 8- and 10-cell geometry. In this case the S_W and H_W parameters were larger than in the 6-cell case, since curved trajectories were more frequent in these stents. For this reason, their value might be increased.

The stents have a mean thickness of 50,25 μm. This thickness is comparable to high-precision stents manufactured with SLA additive manufacturing strategies [10]. High SW thickness has been shown to cause turbulent flow in small arteries. Thus, being one of the main causes of stent restenosis in polymeric stents [26]. Therefore, although S_W values are usually designed above this in commercial stents, their thickness is of great value. For instance, stents manufactured with FDM, which is another material deposition technology, have values in the range of 200 μm, depending on the manufacturing parameters [27]. Then, as the stents manufactured in this study had thinner thickness than those manufactured through comparable methods in the literature, they exhibit significantly lower compression values. For example, when contrasting stents fabricated through SC-DW but using PLLA, notable differences become apparent [28]. In addition, the stent manufactured with polydiolcitrate polymer and fabricated by SLA presented up to 10 times higher compressive strength, comparing the highest results among the studies [7]. Furthermore, PVA stents manufactured through traditional methods such as braiding presented values two orders of magnitude lower than stents fabricated by PVA in this study [18]. However, it is important to note that in all cases the involved stents were thicker, nearly 3 times in each scenario. To further investigate the relationship between thickness and compressive strength, the effect of layering on stent performance is discussed.

The 6-cell stent geometry was studied, which is the one with significantly less material, approximately half of the weight of the 10-cell stents. It was observed that the compressive strength increased almost threefold in the case of 6-cell stents with 2 layers, thus double of thickness. These findings suggest that the impact of thickness on

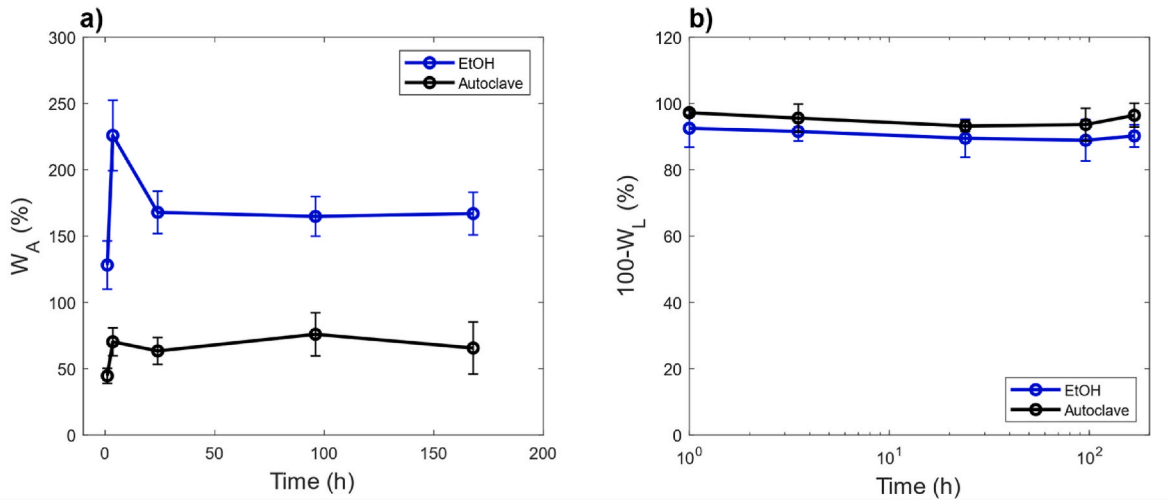

Fig. 10. Degradation Test Data at Time Points: 1 h, 4 h, 1 day, 4 days, and 7 days. A) Water absorption, Eq. (2). B) Weight loss, Eq. (3).

compressive strength is not directly proportional but rather follows an exponential trend. Increasing the thickness enhances the material consistency and subsequently improves the compressive strength, yielding notable mechanical properties to the compression. The results showed that stents with 8- and 10-cell geometries had higher compressive strength than 6-cell geometries. Hence, it is plausible to assume that the growth pattern with the addition of the 2nd layer observed in 6-cell would be reproduced by the 8- and 10-cell geometries, leading to values similar to those presented by similar studies using the SC-DW technology [8]. This observation underlines the importance of the stent geometry in determining its mechanical properties and highlights the potential for further optimization.

Furthermore, it is also important to note the importance of printing on a tubular surface. This prevents stent fabrication from being affected by adhesion of subsequent layers, especially when the stent is subjected to compression. In processes such as FDM, SLA or SLM fabrication or other layering techniques, adjacent layers form small grooves [21,29,30]. The adhesion between these layers induces a staircase effect, causing stress concentration within the grooves. Subsequently, during compression testing, this stress concentration results in the appearance of tiny cracks, which ultimately lead to fracture of the stent support struts and a consequent decrease in mechanical properties [21]. For this reason, a more efficient way to add material and thickness to SC-DW stents, while avoiding layering, would be to increase the concentration of PVA in the solution.

In terms of elastic recovery, it also revealed promising results when a second layer was added. Stents with two layers showed a significant increase in the elastic recovery of 88,85 %, which represents a 35,04 % increase compared to single-layer stents. This suggests that layering significantly influences the ability of the stent to recover its original shape after deployment. The results for the other conditions were lower than 80 %. Assuming an increase in elastic recovery similar than the one observed in the 6 cells stents, a substantial improvement could be expected, possibly leading to an elastic recovery approaching to 100 %.

Additionally, the capacity of over-expansion was analyzed. Cardiovascular stents are designed with the ability to recover their original diameter after crimping during an angioplasty. This is a crucial factor as it ensures a correct placement. However, cardiovascular stents are also intended to be designed so that they can over-expand by at least 0.5 mm of their original diameter to achieve optimal placement [31]. This factor was studied with the fabricated PVA stents. Specifically, 6-cell stents demonstrated a maximum expansion of 130 %. However, the value decreased by approximately 16.26 % after 5 min from the beginning of the test. The 10-cell stents expanded 0.51 mm, but the recoil was significantly greater. Consequently, the overexpansion capacity was lower than expected for a commercial stent. This observation highlights the potential difficulties in maintaining stable expansion with 6-cell and 10-cell stents, which could impact their performance and efficacy in real-world applications. In contrast, the 8-cell stents showed an expansion of 0.87 mm, with practically a negligible recoil at 5 min, resulting in a mean expansion value of 0.8 mm. This behavior suggests that the 8-cell stents effectively retained their expanded state, indicating possible advantages in maintaining proper positioning and vessel support.

4.2. *PVA as a potential material for cardiovascular implants*

In the biomedical engineering field PVA has become a leading and extensively used polymer due to its mechanical properties. Its versatility has made PVA a candidate with good perspectives for the development of a wide range of biomedical applications, due to its properties such as hydrophobicity, biocompatibility and the ability to adapt its mechanical properties to suit specific applications [32]. In particular, PVA can be customized to exhibit very specific properties, such as anisotropy, which shows promising potential for cardiovascular applications [33]. In this direction previous studies have studied the fabrication of PVA stents manufactured by conventional methods, such as braiding or molding in the form of tubes that were then cut into stents [25]. However, the present study presents an innovative approach that to the best of the author's knowledge is the first reported case of a PVA stents fabricated through tubular SC-DW technology.

Since the final product derived from the initial PVA solution can result in different properties depending on the fabrication process, various tests were conducted to assess their impact on the PVA hydrogels manufactured. Specifically, the objective was to evaluate the possibility of controlling the crystallinity of PVA by means of the sterilization process. PVA specimens were prepared by extrusion using SC-DW and subsequently subjected to sterilization. Two sterilization methods were used: autoclaving and ethanol sterilization. After sterilization, the crystallinity of the PVA material was analyzed by DSC. It was found that a substantial increase in crystallinity was observed when the PVA material was autoclaved compared to the ethanol sterilization alternative. This observation aligns with existing literature, which indicates that heating of PVA leads to a gradual loss of water, resulting in a reduction of hydrogen bonds with water molecules. As a consequence, the material undergoes crystallization during the cooling process [34]. Therefore, the control of the temperature during sterilization appeared as a key factor in modulating the crystallinity of PVA. In addition, the increase in crystallinity is attributed to the ability to control other properties. The diminishing of W_A capacity, for instance, holds significant implications for the fabrication of stents [11]. A lower water absorption rate is highly

advantageous in stent applications, as it contributes to the preservation of the mechanical properties of the stent in aqueous environments.

This study hypothesized that the crystallization of PVA hydrogels could be increased with several autoclaving cycles in the same way as occurs with freeze-thaw cycles [35]. The results confirmed the initial hypothesis that multiple autoclaving cycles can indeed increase the crystallinity of PVA. As shown in Fig. 9, the E' increased with each autoclaving iteration, indicating an increase in crystallinity. In addition, a significant reduction in WA was observed, as reported in Fig. 10-a. These results indicate the advantageous effect of autoclave sterilization in the fabrication of stents, showing an increase in PVA crystallinity attributable to this sterilization method, in contrast to ethanol sterilization.

It is noteworthy that in the first iteration of autoclaving the PVA's crystallinity increased by 4,13 % relative to its original state. The subsequent addition of a second autoclaving cycle led to an additional 2.63 % increase in crystallinity over the state reached after the first cycle. This shows that, although autoclaving cycles seem to promote crystallinity, the relationship between the number of cycles and crystallinity does not show a linear growth pattern. While a maximum crystallinity value of 41,33 % was achieved in this study, it is important to acknowledge that PVA can potentially reach a nominal crystallinity value of up to 48,61 % [36]. This implies the feasibility of further increasing the crystallinity by approximately 7 % through additional autoclave cycles, which can effectively improve the mechanical properties of the material while reducing W_A. Nevertheless, the W_A property provided by PVA has been previously employed as a property for self-expandable stents in biliary interventions [25]. While it may not be a primary consideration for cardiovascular stents due to the trade-off between mechanical properties and W_A capacity. It might be relevant to explore this attribute to other stent types, as it may present a valuable solution for specific stenting applications.

In relation to W_L, the stability of PVA in the body has been of interest in biomedical research in the past. Previous studies with fluorescent PVA in mice have demonstrated its remarkable stability, as no traces of PVA were detected in urine or feces [37]. Furthermore, similar to other biocompatible polymers such as PLA, PVA has a relatively low toxicity, whether administered orally or intravenously to the body. After degradation, it is eliminated by biliary excretion [37]. Additionally, very few bioaccumulation and limited adverse effects have been reported, making it ideal for biomedical applications [38].

The results of this study corroborate the idea that PVA is stable in aqueous solutions, such as PBS, since as illustrated in Fig. 10-b, autoclaved and ethanol-sterilized hydrogels showed an initial drop of 6,8 % and 11,1 %, respectively. However, subsequently, a flat pattern was observed indicating that the hydrogel no longer degraded over time. It is worth mentioning that, although the value of the last point is higher than that of the previous ones, due to the flat nature of the pattern, occasionally higher points are expected due to the variability of the experiment. However, it should be noted that the value is lower than the initial weight. Furthermore, the variability found is lower than 2.8 % and 1.3 % of the weight loss for autoclave and EtOH respectively, which is not a significant value, considering that the overall weight loss is 11.1 % for EtOH and 6.8 % for autoclave. The degradation of PVA involves its dissolution in PBS. PVA solubility is affected by factors such as temperature, crystallization rate and the degree of hydrolysis. Studies showed that at temperatures of 40 °C for a PVA of hydrolysis grade similar to the one employed in this study, the solubility in water is 5 % [11]. Therefore, this W_L in the first hours should be attributed to rapid dissolution. Furthermore, the lower crystallinity degree in the ethanol-sterilized hydrogels suggests the existence of larger amorphous regions, possibly explaining a higher dissolution of PVA by this group. Hydrophilic groups in the amorphous regions interact with water molecules, breaking intramolecular hydrogen bonds and accelerating dissolution in the early stages. Our findings are in agreement with Lin et al. which registered a 16 % W_L at 15 days by degrading pure PVA in PBS at 37 °C [16]. In addition, leaching of low molecular weight components, plasticizers, or residual solvents, depending on the PVA formulation or processing methods, should also be taken into account, as it could accentuate this rapid W_L observed in the early stages of the experiment.

Regarding the mechanical properties, this study reveals remarkable findings, particularly for the use of PVA for the manufacture of stents. The reported E′ values for ethanol sterilized PVA hydrogels were found to be similar than those typically observed for materials commonly used for the manufacture of commercial stents. Furthermore, when the mechanical properties of the PVA were increased with 2 autoclaving cycles, it depicted E′ values comparable to sisal fiber reinforced PLA on the surface [39]. This observation is significant since commercial stents on the market are commonly composed of PLLA. The comparable mechanical properties observed between autoclaved PVA and PLLA suggest that PVA is a promising candidate for stent fabrication, providing a viable alternative to traditional PLLA-based stents. Furthermore, the use of autoclaved PVA eliminates the need to remove ethanol, which could present cytotoxic risks if not removed completely, thus eliminating this compound from the manufacturing process. Moreover, PVA exhibits a greater ability to withstand higher temperatures compared to PLLA. Therefore, all the mentioned properties added to this enhanced thermal resilience of PVA further highlights its potential suitability for stent fabrication.

5. Conclusions

This study successfully fabricated PVA stents using SC-DW with different geometries. The optimized printing parameters yielded medical devices with promising dimensional resolution, particularly for straight trajectories. The stents underwent expansion and compression tests, demonstrating favorable stenting kinetics and good over-expansion ability. While the compression performance did not reach excellence, the results were encouraging. In addition, the material was subjected to degradation, crystallinity and mechanical performance tests that demonstrated that there is potential for further improvement of PVA stents. Improving the degree of crystallization by autoclaving improves mechanical properties and decreases water absorption. Therefore, it can be concluded that, for the manufacture of cardiovascular stents, autoclaving produces better results, while simplifying the process by eliminating the need to use ethanol. Finally, the fabricated stents exhibited thinner struts compared to other stents presented in the literature and commercial models. The study has demonstrated that the addition of an extra layer, improved all the stent outcomes. These findings suggest that PVA stents have significant potential for advancements in this medical device technology, thus making the PVA a good candidate to further investigate for the stenting application.

Ethics approval and consent to participate

Not applicable.

Availability of data and materials

Data sets obtained and/or analyzed during the present study are available from the corresponding author upon request.

Funding

This project (BASE3D 001-P-001646) is co-financed by the European Union Regional Development Fund within the framework of the ERDF Operational Program of Catalonia 2014–2020 with a grant of 50 % of total cost eligible. In addition, it was supported by the Generalitat de Catalunya through the PhD student fellowship FI AGAUR. Their financial support played a crucial role in enabling the research activities and data collection necessary for the successful completion of this project.

CRediT authorship contribution statement

Enric Casanova-Batlle: Writing – original draft, Validation, Methodology, Investigation, Formal analysis, Data curation, Conceptualization. **Samuel Montero-Coedo:** Investigation. **Aniol Bosch:** Methodology, Investigation, Conceptualization. **Antonio J. Guerra:** Writing – review & editing, Supervision, Project administration, Methodology. **Joaquim Ciurana:** Writing – review & editing, Resources, Project administration, Funding acquisition, Conceptualization.

Declaration of competing interest

The authors declare that they have no known competing financial interests or personal relationships that could have appeared to influence the work reported in this paper.

Data availability

Data will be made available on request.

Acknowledgements

The authors gratefully acknowledge the support of the Generalitat de Catalunya through the project (BASE3D 001-P-001646) which is co-financed by the European Union Regional Development Fund under the ERDF Operational Program of Catalonia 2014–2020 with a grant of 50 % of the total eligible cost. The authors would also like to thank the Generalitat de Catalunya and the European Union for the predoctoral grant FI AGUR 2021FI_B 00363. Finally, special gratitude to *La granja de la seda* and AERCEGSA for the supply of high quality silk cocoons.

References

[1] P.W. Serruys, M.J.B. Kutryk, A.T.L. Ong, Coronary-Artery Stents, vol. 354, Feb. 2006, pp. 483–495, https://doi.org/10.1056/NEJMRA051091, 5.
[2] A. Colombo, I. Iakovou, Drug-eluting stents: the new gold standard for percutaneous coronary revascularisation, Eur. Heart J. 25 (11) (Jun. 2004) 895–897, https://doi.org/10.1016/J.EHJ.2004.04.004.
[3] H.Y. Ang, H. Bulluck, P. Wong, S.S. Venkatraman, Y. Huang, N. Foin, Bioresorbable stents: current and upcoming bioresorbable technologies, Int. J. Cardiol. 228 (Feb. 2017) 931–939, https://doi.org/10.1016/J.IJCARD.2016.11.258.
[4] N. Muhammad, A.A. Azli, M.S. Saleh, M.N.A. Salimi, M.F. Ghazli, S.Z.A. Rahim, A review on additive manufacturing in bioresorbable stent manufacture, AIP Conf. Proc. 2347 (1) (Jul. 2021), https://doi.org/10.1063/5.0051941/642013.
[5] L. Yang, et al., Additive manufacturing in vascular stent fabrication, MATEC Web of Conferences 253 (2019) 03003, https://doi.org/10.1051/MATECCONF/201925303003.
[6] A. Guerra, A. Roca, J. Ciurana, A novel 3D additive manufacturing machine to biodegradable stents, Procedia Manuf. 13 (2017) 718–723, https://doi.org/10.1016/j.promfg.2017.09.118.
[7] R. Van Lith, et al., 3D-Printing strong high-resolution antioxidant bioresorbable vascular stents, Adv Mater Technol 1 (9) (Dec. 2016) 1600138, https://doi.org/10.1002/ADMT.201600138.
[8] V. Chausse, et al., Solvent-cast direct-writing as a fabrication strategy for radiopaque stents, Addit. Manuf. 48 (Dec. 2021) 102392, https://doi.org/10.1016/J.ADDMA.2021.102392.
[9] L.C. Geng, X.L. Ruan, W.W. Wu, R. Xia, D.N. Fang, Mechanical properties of selective laser sintering (SLS) additive manufactured chiral auxetic cylindrical stent, Exp. Mech. 59 (6) (Jul. 2019) 913–925, https://doi.org/10.1007/S11340-019-00489-0/FIGURES/13.
[10] A. Bosch, E. Casanova-Batlle, I. Constantin, C. Rubio, J. Ciurana, A.J. Guerra, An innovative stereolithography 3D tubular method for ultrathin polymeric stent manufacture: the effect of process parameters, Polymers 15 (21) (Nov. 2023) 4298, https://doi.org/10.3390/POLYM15214298, 2023, Vol. 15, Page 4298.
[11] C.M. Hassan, N.A. Peppas, Structure and applications of poly(vinyl alcohol) hydrogels produced by conventional crosslinking or by freezing/thawing methods, Adv. Polym. Sci. 153 (2000) 37–65, https://doi.org/10.1007/3-540-46414-X_2.
[12] C.M. Hassan, P. Trakampan, N.A. Peppas, Water solubility characteristics of poly (vinyl alcohol) and gels prepared by freezing/thawing processes, Water Soluble Polymers (2002) 31–40, https://doi.org/10.1007/0-306-46915-4_3.
[13] R.V. Gadhave, P.A. Mahanwar, P.T. Gadekar, Effect of glutaraldehyde on thermal and mechanical properties of starch and polyvinyl alcohol blends, Des. Monomers Polym. 22 (1) (Jan. 2019) 164, https://doi.org/10.1080/15685551.2019.1678222.
[14] B. Bolto, T. Tran, M. Hoang, Z. Xie, Crosslinked poly(vinyl alcohol) membranes, Prog. Polym. Sci. 34 (9) (Sep. 2009) 969–981, https://doi.org/10.1016/J.PROGPOLYMSCI.2009.05.003.
[15] K. Pal, A.K. Banthia, D.K. Majumdar, Preparation and characterization of polyvinyl alcohol-gelatin hydrogel membranes for biomedical applications, AAPS PharmSciTech 8 (1) (Mar. 2007), https://doi.org/10.1208/PT080121.
[16] M.C. Lin, C.W. Lou, J.Y. Lin, T.A. Lin, Y.S. Chen, J.H. Lin, Biodegradable polyvinyl alcohol vascular stents: structural model and mechanical and biological property evaluation, Mater. Sci. Eng. C 91 (Oct. 2018) 404–413, https://doi.org/10.1016/J.MSEC.2018.05.030.
[17] W.K. Wan, G. Campbell, Z.F. Zhang, A.J. Hui, D.R. Boughner, Optimizing the tensile properties of polyvinyl alcohol hydrogel for the construction of a bioprosthetic heart valve stent, J. Biomed. Mater. Res. 63 (6) (Jan. 2002) 854–861, https://doi.org/10.1002/JBM.10333.
[18] M.C. Lin, C.W. Lou, J.Y. Lin, T.A. Lin, Y.S. Chen, J.H. Lin, Fabrication of a biodegradable multi-layered polyvinyl alcohol stent, Fibers Polym. 19 (8) (Aug. 2018) 1596–1604, https://doi.org/10.1007/S12221-018-8141-Z/METRICS.
[19] M.S. Utomo, Y. Whulanza, F.P. Lestari, A. Erryani, I. Kartika, N.A. Alief, Determination of compressive strength of 3D polymeric lattice structure as template in powder metallurgy, IOP Conf. Ser. Mater. Sci. Eng. 541 (1) (Jun. 2019) 012042, https://doi.org/10.1088/1757-899X/541/1/012042.
[20] J.C. Flores-Arriaga, D. Chavarría-Bolaños, A. de J. Pozos-Guillén, V.A. Escobar-Barrios, B.I. Cerda-Cristerna, Synthesis of a PVA drug delivery system for controlled release of a Tramadol-Dexketoprofen combination, J. Mater. Sci. Mater. Med. 32 (5) (May 2021), https://doi.org/10.1007/S10856-021-06529-3.
[21] Z. Wu, et al., Radial compressive property and the proof-of-concept study for realizing self-expansion of 3D printing polylactic acid vascular stents with negative Poisson's ratio structure, Materials 11 (8) (2018), https://doi.org/10.3390/MA11081357.
[22] ISO 25539-2:2020 - Cardiovascular implants — Endovascular devices — Part 2: Vascular stents." Accessed: June. 21, 2023. [Online]. Available: https://www.iso.org/standard/69835.html.
[23] E. Polonio-alcalá, et al., Polycaprolactone electrospun scaffolds produce an enrichment of lung cancer stem cells in sensitive and resistant EGFRm lung adenocarcinoma, Cancers 13 (21) (Nov. 2021), https://doi.org/10.3390/CANCERS13215320.
[24] N.A. Peppas, E.W. Merrill, Differential scanning calorimetry of crystallized PVA hydrogels, J. Appl. Polym. Sci. 20 (6) (Jun. 1976) 1457–1465, https://doi.org/10.1002/APP.1976.070200604.
[25] Y. Nagakawa, S. Fujita, S. Yunoki, T. Tsuchiya, S. ichiro Suye, T. Itoi, Self-expandable hydrogel biliary stent design utilizing the swelling property of poly (vinyl alcohol) hydrogel, J. Appl. Polym. Sci. 137 (28) (Jul. 2020) 48851, https://doi.org/10.1002/APP.48851.
[26] A. Sakamoto, H. Jinnouchi, S. Torii, R. Virmani, A.V. Finn, Understanding the impact of stent and scaffold material and strut design on coronary artery thrombosis from the basic and clinical points of view, Bioengineering 5 (3) (Sep. 2018) 71, https://doi.org/10.3390/BIOENGINEERING5030071, 2018, Vol. 5, Page 71.
[27] A.J. Guerra, J. Ciurana, 3D-printed bioabsorbable polycaprolactone stent: the effect of process parameters on its physical features, Mater. Des. 137 (Jan. 2018) 430–437, https://doi.org/10.1016/J.MATDES.2017.10.045.
[28] V. Chausse, C. Iglesias, E. Bou-Petit, M.P. Ginebra, M. Pegueroles, Chemical vs thermal accelerated hydrolytic degradation of 3D-printed PLLA/PLCL bioresorbable stents: characterization and influence of sterilization, Polym. Test. 117 (Jan. 2023) 107817, https://doi.org/10.1016/J.POLYMERTESTING.2022.107817.
[29] A.G. Demir, B. Previtali, Additive manufacturing of cardiovascular CoCr stents by selective laser melting, Mater. Des. 119 (Apr. 2017) 338–350, https://doi.org/10.1016/J.MATDES.2017.01.091.
[30] A.M. Sousa, A.M. Amaro, A.P. Piedade, 3D printing of polymeric bioresorbable stents: a strategy to improve both cellular compatibility and mechanical properties, Polymers 14 (6) (Mar. 2022) 1099, https://doi.org/10.3390/POLYM14061099, 2022, Vol. 14, Page 1099.
[31] J. Ng, et al., Over-expansion capacity and stent design model: an update with contemporary DES platforms, Int. J. Cardiol. 221 (Oct. 2016) 171–179, https://doi.org/10.1016/J.IJCARD.2016.06.097.
[32] G. Rivera-Hernández, M. Antunes-Ricardo, P. Martínez-Morales, M.L. Sánchez, Polyvinyl alcohol based-drug delivery systems for cancer treatment, Int J Pharm 600 (May 2021) 120478, https://doi.org/10.1016/J.IJPHARM.2021.120478.
[33] L.E. Millon, H. Mohammadi, W.K. Wan, Anisotropic polyvinyl alcohol hydrogel for cardiovascular applications, J. Biomed. Mater. Res. B Appl. Biomater. 79B (2) (Nov. 2006) 305–311, https://doi.org/10.1002/JBM.B.30543.
[34] N.A. Peppas, E.W. Merrill, Development of semicrystalline poly(vinyl alcohol) hydrogels for biomedical applications, J. Biomed. Mater. Res. 11 (3) (1977) 423–434, https://doi.org/10.1002/JBM.820110309.
[35] S. Jiang, S. Liu, W. Feng, PVA hydrogel properties for biomedical application, J. Mech. Behav. Biomed. Mater. 4 (7) (Oct. 2011) 1228–1233, https://doi.org/10.1016/J.JMBBM.2011.04.005.
[36] O.W. Guirguis, M.T.H. Moselhey, O.W. Guirguis, M.T.H. Moselhey, Thermal and structural studies of poly (vinyl alcohol) and hydroxypropyl cellulose blends, Nat. Sci. 4 (1) (Dec. 2011) 57–67, https://doi.org/10.4236/NS.2012.41009.
[37] Y. Kaneo, S. Hashihama, A. Kakinoki, T. Tanaka, T. Nakano, Y. Ikeda, Pharmacokinetics and biodisposition of poly(vinyl alcohol) in rats and mice, Drug

Metabol. Pharmacokinet. 20 (6) (Jan. 2005) 435–442, https://doi.org/10.2133/DMPK.20.435.

[38] C.C. DeMerlis, D.R. Schoneker, Review of the oral toxicity of polyvinyl alcohol (PVA), Food Chem. Toxicol. 41 (3) (Mar. 2003) 319–326, https://doi.org/10.1016/S0278-6915(02)00258-2.

[39] Z. Li, X. Zhou, C. Pei, Effect of sisal fiber surface treatment on properties of sisal fiber reinforced polylactide composites, Int J Polym Sci 2011 (2011), https://doi.org/10.1155/2011/803428.